Highly Durable Graphene Monolayer Electrode on Insulating Substrate under Long-term Hydrogen Evolution Cycling

Michel Wehrhold[1], Tilmann J. Neubert[1], Tobias Grosser[1] and Kannan Balasubramanian[1*]

[1]School of Analytical Sciences Adlershof (SALSA), IRIS Adlershof & Department of Chemistry, Humboldt-Universität zu Berlin, Germany.

* *Corresponding author e-mail*: nano.anchem@hu-berlin.de

ABSTRACT

Electrochemical hydrogen evolution reaction (HER) at single graphene sheets has been investigated widely either in its pristine form or after chemical modification. One important challenge is the long-term stability of single graphene sheets on Si/SiO_2 substrates under HER. Previous reports have found that due to stress developing under gas evolution, the sheets tend to break apart, with a very low lifetime limited to just a few cycles of HER. Here, we show through appropriate electrode preparation that it is possible to achieve highly durable single graphene electrodes on insulating substrates, which can survive several hundreds of HER cycles with virtually no damage to the sp^2-carbon framework. Through systematic investigations including atomic force microscopy, Raman spectroscopy and electroanalysis, we show that even after so many cycles, the sheet is physically intact and the electron transfer capability of the electrodes remain unaffected. This extremely high stability of a single atomic sheet of carbon, when combined with appropriate chemical modification strategies, will pave way for the realization of novel 2D electrocatalysts.

Keywords: graphene monolayer, hydrogen evolution, HER

INTRODUCTION

Single sheets of 2D materials, such as graphene, in pristine or modified form are emerging to be promising candidates for electrocatalysis. In its pristine form, several electrochemical reactions have been studied at graphene such as the hydrogen evolution reaction (HER). [1-5] The sp^2-conjugated carbon network is a rather poor electrocatalyst for HER, due to the unfavorable adsorption energy of solvated protons on to pristine graphene. [6] However, chemical modification of graphene sheets and hybrid structures comprised of graphene sheets can allow to reduce the overpotential for HER. [7] Moreover, single graphene sheets supported on noble or non-noble metal layers were found to exhibit good HER activity, sometimes approaching that of the crystalline Pt (111) surface. [8, 9] On the other hand, heteroatom doping of carbon nanosheets has been shown to deliver electrocatalytic properties, raising hopes of metal-free carbonaceous catalysts. [10, 11] It has also been theoretically proposed that introducing defects [12] or varying the doping level of graphene [6, 9] may allow for improved hydrogen adsorption thereby enhancing HER.

One of the fundamental challenges, for the widespread use of graphene as an electrocatalyst, concerns the maintenance of the durability of the electrode comprised of just a single sheet of carbon atoms. It has been shown that HER can be observed on as-prepared monolayer graphene on an insulating substrate such as Si/SiO_2. [2, 3] However, already after three cycles, the sheet was found to break apart, due to large hydrogen bubbles emanating from the HER. [2] Even in few layer graphene, it was found that the integrity of the sp^2-carbon framework is compromised upon HER cycling. [2] When a graphene sheet is supported on a metal substrate (e.g. Pt, Au, Fe), HER is enhanced. One mechanism that has been discussed in this context is the possibility of protons to penetrate through the graphene layer, either directly or through single point defects, [13, 14] and subsequently be reduced at the underlying metal electrode. In this scenario, the formation of hydrogen bubbles below the graphene sheet may lead to delamination causing physical changes of the graphene sheet. [4, 15] Hence, for graphene to be usable as a good

candidate for electrocatalysis, it is important that the electrode is durable under continuous gas evolution. Also with an underlying metal surface, introduction of structural defects on graphene has been proposed as a way to favor hydrogen evolution. [4] On single crystalline Pt(111) electrodes, graphene was found to be extremely stable even after performing thousand cycles of HER. [5, 9] It should be noted that in the last two cases, graphene was directly synthesized on the Pt(111) crystal, in contrast to other graphene monolayer electrodes, which are typically chemical vapor deposition (CVD)-grown and are subsequently transferred to a desired substrate.

In this work, we focus on single CVD-grown graphene sheets on an insulating SiO_2 substrate and show that we can indeed realize graphene electrodes that show a high stability to HER for numerous cycles in three different acid solutions: HCl, $HClO_4$ and H_2SO_4. Specifically, we use an optimized preparation strategy, [16, 17] which involves metal-ion-free etching of the copper substrate followed by an annealing and electrochemical etching step [18] to prepare intact single layer graphene electrodes mostly free of trace metal impurities. A graphene sheet prepared in this manner is very stably held on the insulating SiO_2 substrate. Using this elaborate preparation strategy, we observe that the electrodes can easily withstand at least 1000 cycles of HER in $HClO_4$ without undergoing any structural damage. Through systematic characterization using optical microscopy, atomic force microscopy (AFM) and Raman spectroscopy, we show that the HER cycling does not increase the defect density in the sp^2-carbon framework. Most importantly, the layer is found to be intact without any cracks or holes. Furthermore, through electroanalysis, we show that the electron transfer characteristics to a classical redox probe ferrocenedimethanol remain unaffected even after the prolonged HER cycling experiments.

RESULTS AND DISCUSSION

Graphene monolayer electrodes were prepared according to a fabrication strategy that we have outlined in our previous works. [17] Specifically, we use polystyrene as a polymer support to coat

commercially obtained graphene on copper foils. The copper is etched away in an acidified peroxide solution, followed by transfer of the polystyrene-graphene stack on to a Si/SiO_2 substrate with pre-fabricated platinum contacts (see *Methods* in SI for details). The polystyrene is stripped away in toluene. In order to avoid any trapped water below graphene [19] and to obtain a maximal conformal contact with the underlying substrate, the samples are annealed in N_2 atmosphere at 600°C. The platinum contacts are passivated with a resin in order to ensure that only the graphene sheet is in contact with the solution. Following this, we perform an electrochemical etching step [18] to get rid of trace metal impurities, which may parasitically catalyze HER and may lead to unwanted damage of the graphene sheet. The graphene electrodes prepared in this manner were found to be extremely stable to HER as discussed below.

The stability was evaluated by cycling the potential in 0.1 M $HClO_4$ to promote hydrogen evolution. Figure 1a shows selected cyclic voltammograms (CVs) in perchloric acid obtained at a typical graphene electrode, at which 100 cycles were performed. Here the evolution of hydrogen can be inferred from the high current density at the extreme cathodic potentials. Our graphene monolayer electrodes show an overpotential for HER in the range of −0.42 to −0.47 V (vs. NHE, Normal Hydrogen Electrode) at a current density of 0.1 mA cm^{-2}. This overpotential and the magnitude of the observed current density at an overpotential of −1 V vs. NHE are similar to what has been observed on graphene on copper electrodes. [3] The onset potential for HER has been reported to be sensitive to substrate-induced doping of graphene. At these cathodic potentials, we also observe bubble formation (see figure S1 in SI and supporting video). The magnitude of the current due to HER and the onset potential show only little changes during the cycling. The slight cycle-to-cycle variation is attributed to H_2 bubble formation on the electrode surface, which causes some noise in the current measurement. To examine the structural stability, atomic force microscopy (AFM) was carried out on the same electrode before and after performing HER. Figure 1b shows an AFM image of an electrode

region before HER. A height of <1 nm can be extracted for graphene from line profiles, with a few wrinkles and cracks observable, which are typical for CVD-grown graphene on SiO_2. Figure 1c displays an AFM image of the same position after the HER cycling, which shows that the graphene sheet remains completely intact after the 100 cycles of HER. No additional cracks, holes or even roll-up of graphene was introduced by the cycling. We can see that the graphene monolayer surface was even more clean after the HER cycling through the removal of some surface contamination. This is a tremendous improvement (see another example in figure S2 in SI) in comparison to previous work showing that monolayer graphene was already destroyed after the first two cycles of HER. [2] Similar performance was also observed at the fabricated graphene electrodes in HCl and H_2SO_4 solutions (see figure S3 in SI).

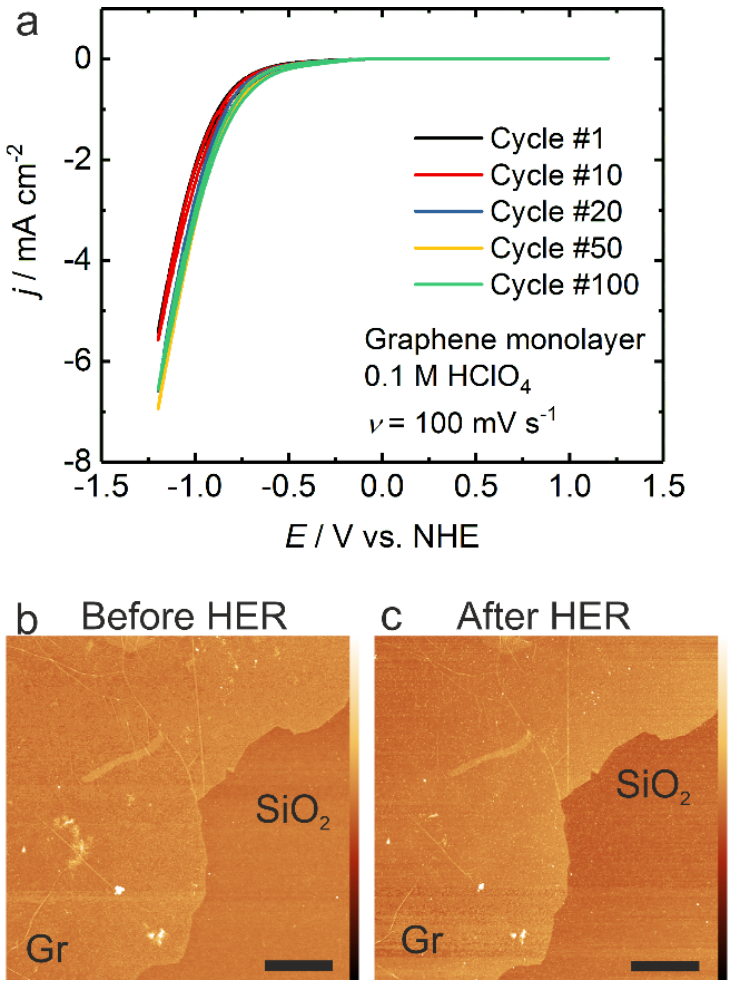

Figure 1. (a) Cyclic voltammograms (selected cycles) measured in $HClO_4$ at a graphene electrode on Si/SiO_2 during a 100-cycle HER experiment. j: current density, E: applied potential. (b,c) AFM images of the region of the graphene (Gr) monolayer electrode before (b) and after (c) HER cycling. Lateral scale: 2 µm. Height scale: 20 nm.

To understand and determine the limits of stability of our graphene monolayer electrodes, two series of experiments were carried out. In a first series, we wanted to test the maximum number of cycles of HER that graphene can withstand, while in the second series, we decided to test the limit of the extreme vertex potential to which graphene can be polarized without undergoing damage. In the first series, we found out that graphene can easily withstand at least a 1000 cycles of continuous HER cycling. Figure 2a shows CVs measured at the first and 1000^{th} cycle during such an experiment, while figure 2b presents a color map of the current measured during the entire HER cycling. It is quite clear that there is little change in the current density or onset potential during or after the cycling. On this electrode, we have evaluated the integrity of the graphene sheet by measuring the electron transfer properties to a classical redox probe (ferrocenedimethanol - FDM). Figure 2c presents CVs of FDM at this electrode before and after performing the 1000 cycles of HER. The magnitude of the current and the peak potentials are unaffected through the extensive HER cycling experiment. The structural integrity of the sheet is further attested by optical images (see figure 2d) obtained before and after the 1000-cycle-HER, where no new cracks, holes or folds are visible (see further examples in figure S4 in SI). In the second series of experiments with varying vertex potential, we found that our electrodes survive cathodic potentials at least up to -1.5 V vs NHE (in contrast to -1.3 V vs NHE in previous works [2, 3]) without any damage to the graphene sheet (see figures S5 and S6 in SI and associated discussion). Overall, the data indicate that the graphene monolayer electrodes are surviving the excessive electrochemical HER cycling in $HClO_4$ as well as in HCl and H_2SO_4.

In order to obtain an idea of the efficiency of hydrogen evolution on graphene, we have performed a Tafel analysis of the data obtained through the CVs (see figure S7a in SI for a complete profile of Tafel slopes). We extract Tafel slope in the range of 320-470 mV dec^{-1}, which indicates a rather sluggish and slow hydrogen evolution at our graphene monolayer electrodes compared to classical Pt electrodes or graphene supported on metals. This is not

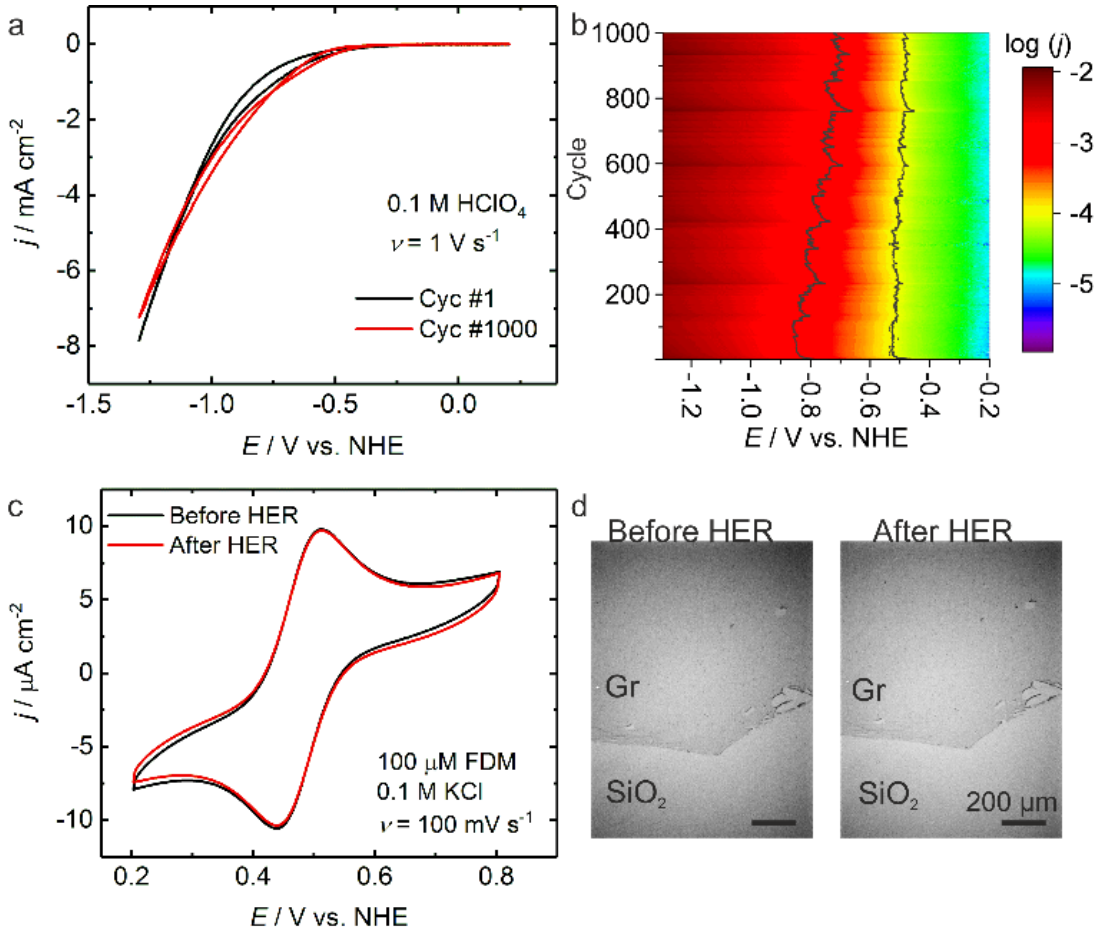

Figure 2. (a) Comparison of the first (black) and last (red) CV cycles of a 1000-cycle HER experiment at graphene. (b) The current density (j, in A cm^{-2}) measured through the entire 1000 cycles is presented as a heat map (log scale). The lines in the map indicate contours of constant current density of 0.1 mA cm^{-2} and 1 mA cm^{-2}. (c) Redox behavior of ferrocenedimethanol (FDM) measured by CV before (black) and after (red) the 1000 cycles of HER at the graphene electrode. (d) Optical images of the same area of the graphene (Gr) monolayer electrode before (left) and after (right) HER cycling.

surprising since the adsorption of the protons on to pristine graphene has a very high energy barrier. [6] Our Tafel slope values are much higher than the values obtained at graphene on copper. [3] There, the underlying copper is expected to catalyze HER on graphene through several possible mechanisms, such as change in surface adsorption energy of protons or holes on graphene or permeability of graphene to protons. [4, 6, 9] In our case, we do not have any metal below graphene and hence we do not expect to have enhanced HER. Our values are also higher than previous reports [2, 3] of graphene on SiO_2 by around 100 mV dec^{-1}. In contrast to the transfer method used there, we use a metal-ion free etching solution followed by an electrochemical etching step, which ensures that we have nearly no trace metal impurities in our samples. Such trace metal impurities could catalyze HER, [18, 20] if not removed properly and may result in lower

Tafel slopes. In fact, the values reported there are between our values and those for graphene on copper. Moreover, we ensure that we have a high proportion of sp^2-carbon, as confirmed by our previous XPS measurements. [17] In our case, this is achieved by the annealing procedure, which minimizes organic contamination. We have also extracted a measure of the exchange current density in our electrode (see figure S7b in SI), which lies in the range of 4-10 μA cm^{-2}. If we assume that the HER undergoes a mechanism similar to that on metals, [21] we can estimate a proton adsorption energy of around 45 kcal mol^{-1}, which is close to the theoretically estimated hydrogen adsorption energy for graphene. [6]

To gather further support for the high structural integrity of our graphene electrodes under HER, we have carried out detailed Raman spectroscopic analysis on our electrodes before and after the electrochemical cycling measurements. Figure 3a presents typical confocal Raman spectra obtained at a specific location in the device of figure 1 in its initial state and after 200 cycles of the electrochemical measurements. Raman peaks characteristic of monolayer graphene – *D*-, *G*- and *2D*-peaks – are unambiguously identifiable in the spectra. We observe a strong *2D*-peak approx. twice as high in intensity as the *G*-peak, which is typical for our as-prepared samples. The acquisition time was set high enough in these measurements to accumulate enough counts in order to observe the *D*-peak with a sufficient resolution, since the relative intensity of this peak (I_D/I_G) gives us an idea about the defect density in the graphene sheet. [22] It is clear that there is virtually no difference in the Raman spectrum before and after HER. In order to obtain statistically significant information, Raman spectra were collected as maps of 5 by 5 spots with a spacing of 5 μm at several locations before and after HER experiments. Parameters such as the relative intensities of the *D*- and *2D*-peak (normalized to the *G*-peak) and the positions of the three peaks were extracted from such spectra. Figure 4b presents a histogram of the observed I_D/I_G ratios before and after the HER cycling experiments. It can be inferred here that there is nearly no change in this ratio signifying a negligibly small change in the density of defects after the HER cycling experiments. This is quite remarkable considering that we have performed

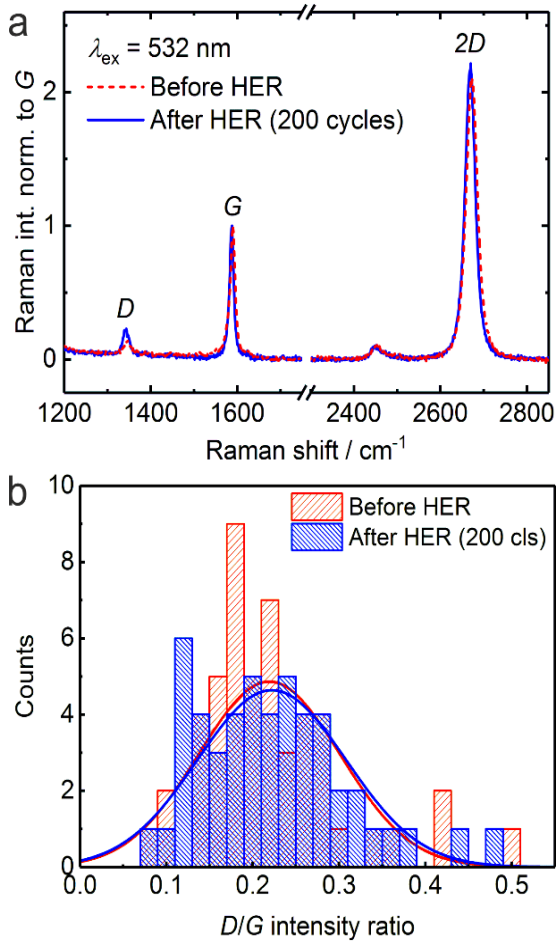

Figure 3. (a) Representative Raman spectra from the same location of a graphene monolayer electrode before and after 200 cycles of HER. The spectra are normalized to the intensity of the G-peak. (b) Histogram of the ratio of D-to-G peak intensity extracted from Raman spectra measured at 50 different locations of a graphene electrode before and after 200 cycles of HER. Every solid curve is a fit to a normal distribution.

several 100 cycles of HER using the one-atom-thick electrode. Typically for defective or covalently modified graphene the *D*-to-*G*-peak intensity ratio (I_D/I_G) is close to or larger than one, [23] which is clearly not the case here. Furthermore, the ratio of the *2D*-to-*G* peak intensity and the positions of the *D*-, *G*- and *2D*-bands are nearly unaffected (within the instrument resolution of ±3 cm^{-1}) by the HER experiments (see figure S8 in SI).

CONCLUSIONS

In conclusion, we can say that careful preparation can indeed allow the repeated use of graphene electrodes for HER on Si/SiO_2 substrates. It is known in carbon research that the preparation of

the electrode has a strong effect on the ensuing electrochemical characteristics. [17, 24, 25] This is in contrast to non-crystalline metal electrodes, where polycrystalline or amorphous planar electrodes give similar electrochemical behavior rather independent of the preparation strategy. This work underlines the necessity to perform sample preparation carefully in order to assess the maximum achievable performance. Here, we could successfully present graphene monolayer electrodes with ultra-high chemical and mechanical stability towards electrochemical HER cycling. Starting out with such electrodes, through appropriate chemical modification, we can reliably fabricate novel electrodes for HER as well as for other electrocatalytic applications.

Supporting Information

Supporting information available

AUTHOR INFORMATION

Corresponding Author

nano.anchem@hu-berlin.de

Funding Sources

Funding from the German Science Foundation (DFG) as part of the excellence initiative *via* the Graduate School of Analytical Sciences Adlershof (GSC1013 SALSA) and *via* grant INST 276/754-1 is gratefully acknowledged.

Acknowledgements

We thank Stephan Schmid and Birgit Lemke from MPI Stuttgart for help with metal deposition and Gina-Maria Erler and Michael Winterfeld from HU Berlin and Martin Muske form HZB for assistance with sample fabrication.

Conflict of Interest

The authors declare no conflict of interest.

REFERENCES

1. J. Li, Z. Zhao, Y. Ma and Y. Qu, *ChemCatChem*, 2017, **9**, 1554-1568.
2. A. García-Miranda Ferrari, D. A. C. Brownson and C. E. Banks, *Sci. Rep.*, 2019, **9**, 15961.
3. A. Xie, N. Xuan, K. Ba and Z. Sun, *ACS Appl. Mater. Interfaces*, 2017, **9**, 4643-4648.
4. A. J. Shih, N. Arulmozhi and M. T. M. Koper, *ACS Catalysis*, 2021, **11**, 10892-10901.
5. Y. Fu, A. V. Rudnev, G. K. H. Wiberg and M. Arenz, *Angew. Chem. Int. Ed.*, 2017, **56**, 12883-12887.
6. E. Santos and W. Schmickler, *J. Phys.: Condens. Matter*, 2021, **33**, 504001.
7. B. Xia, Y. Yan, X. Wang and X. W. Lou, *Materials Horizons*, 2014, **1**, 379-399.
8. K. Hu, T. Ohto, Y. Nagata, M. Wakisaka, Y. Aoki, J.-i. Fujita and Y. Ito, *Nat. Commun.*, 2021, **12**, 203.
9. T. Kosmala, A. Baby, M. Lunardon, D. Perilli, H. Liu, C. Durante, C. Di Valentin, S. Agnoli and G. Granozzi, *Nature Catalysis*, 2021, **4**, 850-859.
10. K. Qu, Y. Zheng, X. Zhang, K. Davey, S. Dai and S. Z. Qiao, *ACS Nano*, 2017, **11**, 7293-7300.
11. Y. Zheng, Y. Jiao, L. H. Li, T. Xing, Y. Chen, M. Jaroniec and S. Z. Qiao, *ACS Nano*, 2014, **8**, 5290-5296.
12. H. Kawabata and H. Tachikawa, *Jpn. J. Appl. Phys.*, 2020, **59**, 025508.
13. J. L. Achtyl, R. R. Unocic, L. Xu, Y. Cai, M. Raju, W. Zhang, R. L. Sacci, I. V. Vlassiouk, P. F. Fulvio, P. Ganesh, D. J. Wesolowski, S. Dai, A. C. T. van Duin, M. Neurock and F. M. Geiger, *Nat. Commun.*, 2015, **6**, 6539.
14. Y. An, A. F. Oliveira, T. Brumme, A. Kuc and T. Heine, *Adv. Mater.*, 2020, **32**, 2002442.
15. S. Yasuda, K. Tamura, T.-o. Terasawa, M. Yano, H. Nakajima, T. Morimoto, T. Okazaki, R. Agari, Y. Takahashi, M. Kato, I. Yagi and H. Asaoka, *The Journal of Physical Chemistry C*, 2020, **124**, 5300-5307.
16. T. J. Neubert, M. Wehrhold, N. S. Kaya and K. Balasubramanian, *Nanotechnol.*, 2020, **31**, 405201.
17. M. Wehrhold, T. J. Neubert, A. Yadav, M. Vondráček, R. M. Iost, J. Honolka and K. Balasubramanian, *Nanoscale*, 2019, **11**, 14742-14756.
18. R. M. Iost, F. N. Crespilho, L. Zuccaro, H. K. Yu, A. M. Wodtke, K. Kern and K. Balasubramanian, *ChemElectroChem*, 2014, **1**, 2070-2074.
19. O. Ochedowski, B. K. Bussmann and M. Schleberger, *Sci. Rep.*, 2014, **4**, 6003.
20. L. J. A. Macedo, R. M. Iost, A. Hassan, K. Balasubramanian and F. N. Crespilho, *ChemElectroChem*, 2019, **6**, 31-59.
21. P. Quaino, F. Juarez, E. Santos and W. Schmickler, *Beilstein Journal of Nanotechnology*, 2014, **5**, 846-854.
22. L. G. Cançado, A. Jorio, E. H. M. Ferreira, F. Stavale, C. A. Achete, R. B. Capaz, M. V. O. Moutinho, A. Lombardo, T. S. Kulmala and A. C. Ferrari, *Nano Lett.*, 2011, **11**, 3190-3196.
23. J. M. Englert, P. Vecera, K. C. Knirsch, R. A. Schäfer, F. Hauke and A. Hirsch, *ACS Nano*, 2013, **7**, 5472-5482.
24. P. R. Unwin, A. G. Güell and G. Zhang, *Acc. Chem. Res.*, 2016, **49**, 2041-2048.
25. A. Yadav, M. Wehrhold, T. J. Neubert, R. M. Iost and K. Balasubramanian, *ACS Applied Nano Materials*, 2020, **3**, 11725-11735.